

Synthesis, crystal structure and molecular modeling of aquo magnesium tetra(methoxyphenyl)porphyrin

Shumei Yang and Robert A. Jacobson*

Ames Laboratory and the Department of Chemistry, Iowa State University, Ames, IA 50011 (USA)

(Received March 6, 1991; revised July 24, 1991)

Abstract

5,10,15,20-Tetrakis(4-methoxyphenyl)porphyrin magnesium(II) monohydrate, $(\text{H}_2\text{O})\text{MgT}(\text{OME})\text{PP}$, has been synthesized. An X-ray structure determination was carried out for $(\text{H}_2\text{O})\text{MgT}(\text{OME})\text{PP} \cdot \text{HCCl}_3$. The crystals are monoclinic, space group $I2$, with cell parameters $a = 15.966(5)$, $b = 9.192(1)$, $c = 14.882(4)$ Å and $\beta = 100.38(2)^\circ$. The structure was solved by direct method and refined to $R = 0.068$ and $R_w = 0.070$ for 1297 observed reflections measured by diffractometer. The unit cell contains two molecules requiring that the molecule possess two-fold crystallographic symmetry. Intermolecular hydrogen bonding results in the formation of two-dimensional infinite polymers; such an occurrence in this structure provides the further support for a model of chlorophyll aggregation in photosynthetic organisms. In addition, molecular mechanics calculations on this compound gave a result in good agreement with the crystal structure determination and showed that the hydrated complex has a lower energy than its non-hydrated counterpart.

Introduction

The structures of magnesium-containing porphyrins are of considerable interest because of their relationship to chlorophyll and its related compounds; detailed knowledge of such structures can aid in the understanding of photosynthesis spectroscopy and its relation to pigment arrangement. The structure of ethyl chlorophyllide *a* dihydrate has been used as a model for the different spectral forms of chlorophyll [1]. It has been proposed that bacteriochlorophyll *c* oligomers (extracted from Chlorobiaceae) are a good model for BChl *c* in the antennae of green bacteria [2–4]. In order to obtain further structural data on Mg-porphyrin compounds which can be used to provide additional insight on chlorophyll aggregation *in vivo*, we chose $\text{H}_2\text{T}(\text{OME})\text{PP}$, an oxygen containing porphyrin, as a ligand, synthesized $(\text{H}_2\text{O})\text{MgT}(\text{OME})\text{PP}$, and determined the crystal and molecular structure of $(\text{H}_2\text{O})\text{MgT}(\text{OME})\text{PP} \cdot \text{HCCl}_3$. The intermolecular hydrogen bonding observed in this structure gives further insight to help explain the chlorophyll aggregation *in vivo*.

Experimental

5,10,14,20-Tetrakis(4-methoxyphenyl)-21H,23H-porphine (97%), $\text{H}_2\text{T}(\text{OME})\text{PP}$, was purchased from Aldrich Chemical Company. All other reagents were of analytical grade.

The magnesium(II) complex was prepared by using Adler's method [5]. Approximately 100 ml of *N,N'*-dimethylformamide was brought to reflux temperature in a flask on a stirring hot plate. Then 0.238 g of $\text{H}_2\text{T}(\text{OME})\text{PP}$ was added. After the porphyrin had dissolved completely, ten times the stoichiometric amount of MgCl_2 (0.3 g) was added. Three hours later, the reaction was checked by UV spectrometry. In contrast to Alder's earlier findings with other porphyrins, the free porphyrin's red fluorescence was still significant. Another 0.1 MgCl_2 was added and the reaction continued overnight. Completion of the reaction was verified spectrophotometrically. After concentration of the solution's volume to 10 ml, 200 ml of water was added. The suspension was filtered through a celite pad, washed with water, and dried. The product was washed from the celite with CHCl_3 and evaporated to dryness. Finally the product was purified by column chromatography on Al_2O_3 with CHCl_3 ; removal of the solvent under reduced pressure yielded 0.17 g purple solid. Purity of the complex was checked by its ^1H NMR spectrum.

*Author to whom correspondence should be addressed.

TABLE 1. Crystallographic data for $(\text{H}_2\text{O})\text{MgT}(\text{OMe})\text{PP}\cdot\text{HCCl}_3$

Empirical formula	$\text{MgO}_5\text{N}_4\text{C}_{49}\text{H}_{39}\text{Cl}_3$
Formula weight	894.53
Crystal color, habit	purple, platelet
Crystal dimensions (mm)	$0.350 \times 0.300 \times 0.300$
Crystal system	monoclinic
No. reflections used for unit cell determination (2θ range)	25 (22.5–39.3°)
Omega scan peak width at half-height	0.41
Lattice parameters	
<i>a</i> (Å)	15.966(5)
<i>b</i> (Å)	9.192(1)
<i>c</i> (Å)	14.882(4)
β (°)	100.38(2)
<i>V</i> (Å ³)	2148.2(9)
Space group	<i>I</i> 2 (No. 5)
<i>Z</i> value	2
<i>D</i> _{calc} (g cm ⁻³)	1.195
<i>F</i> ₍₀₀₀₎	808
μ (Mo <i>K</i> α) (cm ⁻¹)	0.86
Diffractometer	Rigaku AFC6R
Radiation	Mo <i>K</i> α ($\lambda = 0.71069$ Å)
Temperature (°C)	-80
Crystal to detector distance (cm)	40
Scan type	$\omega - 2\theta$
Scan rate (°/min)	16.0 (in omega) (2 rescans)
Scan width (°)	$(1.31 + 0.30 \tan\theta)$
$2\theta_{\text{max}}$ (°)	65.2°
No. reflections measured: total, unique	4614, 4454 (<i>R</i> _{int} = .102)
Corrections	Lorentz-polarization absorption (trans. factors: 0.96–1.00)
Structure solution	direct methods
Refinement	full-matrix least-squares
Function minimized	$\sum w(F_o - F_c)^2$
Least-squares weights	$4F_o^2/\sigma^2(F_o^2)$
<i>p</i> Factor	0.03
Anomalous dispersion	All non-hydrogen atoms
No. observations ($I > 3.00\sigma(I)$)	1297
Residuals: <i>R</i> ; <i>R</i> _w	0.068; 0.070
Max., min. Peak in final difference map (e ⁻ /Å ³)	0.37, -0.37

A single crystal of $(\text{H}_2\text{O})\text{MgT}(\text{OMe})\text{PP}\cdot\text{HCCl}_3$ suitable for X-ray structure determination was grown by slow diffusion of octane into a saturated CHCl_3 solution of $(\text{H}_2\text{O})\text{MgT}(\text{OMe})\text{PP}$.

A purple crystal having approximate dimensions of $0.35 \times 0.30 \times 0.30$ mm was mounted on a glass fiber using epoxy cement and attached to a standard goniometer head. X-ray intensity data were collected at -80 °C on a four-circle RIGAKU X-ray diffractometer using graphite-monochromated Mo *K*α radiation from a rotating anode source. Three standard reflections were monitored every 150 reflections measured, and their intensities showed good stability of the complex throughout data collection. The unit cell was found to be monoclinic, and lattice constants were determined to be $a = 15.966(5)$, $b = 9.192(1)$,

$c = 14.882(4)$ Å, $\beta = 100.38(2)^\circ$ from least-squares refinement of the positions of 15 high angle reflections. A total of 4614 intensities was measured, corresponding to those in the two octants (*hkl*, *hk \bar{l}*) with maximum 2θ value of 65.2°, and 1297 unique 'observed' reflections having $I > 3\sigma(I)$ were used in the structure determination and refinement. Further details are given in Table 1.

Structure analysis

The only observed extinctions were: *hkl*, $h + k + l = 2n + 1$; this is consistent with space groups *I*2, *Im* or *I*2/*m*. Since two molecules per cell is indicated by density considerations, choice of one of those three space groups would require *C*₂, *C*_s

or C_{2h} molecular symmetry. A direct method program [6] was used to determine the structure in each of the three space groups. The best result was obtained in space group $I2$, as the positions of the phenyl groups were found to deviate appreciably from the plane of the porphyrin and the position of the magnesium was found to be displaced above the porphyrin plane.

The structure was then refined using successive least-squares computations with intermediate difference electron density calculations. Full-matrix least-squares refinement with all atoms isotropic yielded a crystallographic residual of $R=0.17$. A subsequent structure factor and electronic density map calculation showed additional atom peaks which appeared to result from the inclusion of a CHCl_3 solvent molecule (disordered) in the crystal. Addition of these atoms reduced R to 0.11. Anisotropic refinement brought the R value down to 0.08. Hydrogen atoms were partially located on a difference Fourier map and partially included from ideal position calculations. The final value of R was 0.068 and R_w was 0.070, with shifts to parameter ratio of less than 0.11. The maximum peak in the final electron density map was $0.37 \text{ e}^-/\text{\AA}^3$. Neutral atom scattering factors were taken from the International Tables for X-ray Crystallography and modified for the real and imaginary parts of anomalous scattering [7–9]. All calculations were performed on a VAX computer using the programs TEXSAN [6] for structure solution, refinement and least-squares plane calculations, and ORTEP for drawing molecular diagrams.

Molecular mechanics calculations

An independent calculation of the molecular structure was carried out using a molecular mechanics program [10]. The porphyrin moiety was sketched in on the computer screen and the magnesium atom was placed at the center of the ligand, albeit with a small out of plane displacement. A water molecule was placed above the magnesium to complete the square pyramid geometry around the metal. The atomic positions were then allowed to adjust using essentially an MM2 algorithm [11] to minimize the energy. In order to be reasonably confident that the result did not correspond to merely a local minimum, the process was repeated a number of times using different starting configurations.

Two alternate starting conformations were also tested. The first had the same atomic configuration as noted above but with the omission of the water molecule. The other conformation also omitted the water molecule and placed the magnesium atom in the plane of the porphyrin ring. In both cases the minimized energy was significantly higher than for the five-coordinate model.

Discussion

Crystal structure

The molecular structure of $(\text{H}_2\text{O})\text{MgT}(\text{OME})\text{PP}$ as determined from the X-ray diffraction analysis is shown in Fig. 1; the fractional coordinates are given in Table 2 and selected bond distances and angles are given in Table 3. The complex has crystallographic C_2 symmetry. The porphyrin core is non-planar. The average dihedral angle between the mean planes of adjacent pyroles is 2.9° . The five-coordinate magnesium atom is displaced 0.39 \AA out of the plane of the central nitrogen atoms toward the water molecule, which is typical in chlorophyll derivatives, a little longer than the 0.23 \AA found in $(\text{H}_2\text{O})\text{MgTPP}$. The bond distance between Mg and the water O is $2.078(12) \text{ \AA}$, and the Mg–N bond distance is also $2.084(7) \text{ \AA}$, similar to those found in $(\text{H}_2\text{O})\text{MgTPP}$ [12]. The average N–Mg–N bond angle is 88° , while the O–Mg–N bond angles range from 99.1 – 103.0° , all of which indicate an essentially square pyramid environment about the Mg. The two phenyl rings are not perpendicular to the porphyrin ring, the dihedral angle between the phenyl plane and the porphyrin plane being approximately 69° , in contrast to $(\text{H}_2\text{O})\text{MgTPP}$ in which the phenyl plane is found to be perpendicular to the porphyrin plane.

The oxygen (O1) in the coordinated water is hydrogen bonded to the methoxyl oxygens (O2) in adjacent molecules (O1 being on the two-fold axis with O1–O2 distance of 2.86 \AA). The intermolecular hydrogen bonds result in the formation of a two-

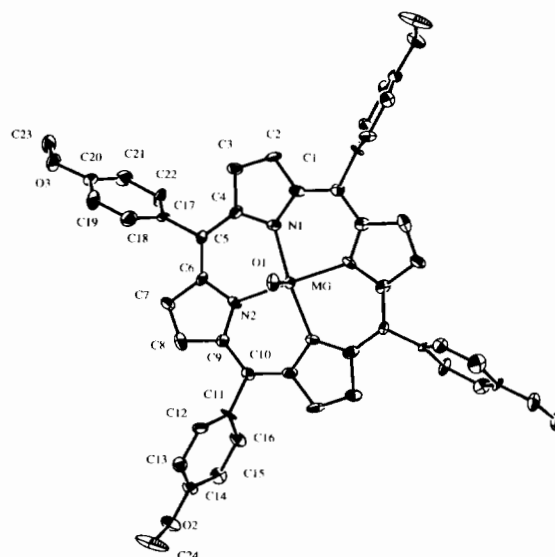


Fig. 1. The molecular structure of $(\text{H}_2\text{O})\text{MgT}(\text{OME})\text{PP} \cdot \text{HCCl}_3$. Hydrogen atoms and solvate molecules have been omitted for clarity. Thermal ellipsoids are drawn at the 50% probability level.

TABLE 2. Positional parameters and B_{eq} for $(\text{H}_2\text{O})\text{-MgT}(\text{OMe})\text{PP}\cdot\text{HCCl}_3$

Atom	x	y	z	B_{eq}^a
Mg	0	0.6403	0	1.3(2) ^b
O(1)	0	0.866(1)	0	2.3(5)
O(2)	-0.5214(4)	0.584(1)	-0.3690(4)	2.6(3)
O(3)	0.2447(4)	0.581(1)	-0.5073(4)	2.7(3)
N(1)	0.1215(4)	0.589(1)	-0.0233(5)	1.7(3)
N(2)	-0.0448(4)	0.604(1)	-0.1389(5)	1.4(3)
C(1)	-0.1945(6)	0.583(2)	-0.0417(7)	1.7(4)
C(2)	0.2672(6)	0.569(2)	-0.0030(7)	2.1(5)
C(3)	0.2392(6)	0.575(2)	-0.0952(7)	1.8(4)
C(4)	0.1471(6)	0.584(2)	-0.1064(6)	1.9(4)
C(5)	0.0926(5)	0.593(1)	-0.1924(5)	1.2(4)
C(6)	0.0042(6)	0.598(1)	-0.2065(6)	1.5(4)
C(7)	-0.0504(6)	0.591(2)	-0.2943(6)	1.9(4)
C(8)	-0.1316(6)	0.596(2)	-0.2778(6)	2.1(4)
C(9)	-0.1276(6)	0.599(1)	-0.1813(6)	1.4(4)
C(10)	-0.1989(5)	0.592(1)	-0.1365(6)	1.4(4)
C(11)	-0.2854(5)	0.592(2)	-0.1955(6)	1.8
C(12)	-0.3159(6)	0.715(1)	-0.2454(7)	1.8(5)
C(13)	-0.3951(6)	0.720(1)	-0.3043(7)	1.9(5)
C(14)	-0.4443(6)	0.596(2)	-0.3099(6)	1.8(4)
C(15)	-0.4173(7)	0.473(1)	-0.2611(7)	1.9(5)
C(16)	-0.3380(7)	0.471(1)	-0.2033(7)	2.0(5)
C(17)	0.1332(5)	0.585(2)	-0.2749(6)	1.4(4)
C(18)	0.1288(7)	0.706(1)	-0.3341(7)	2.4(5)
C(19)	0.1661(8)	0.697(1)	-0.4100(7)	2.8(6)
C(20)	0.2094(6)	0.574(2)	-0.4298(6)	1.6(4)
C(21)	0.2139(7)	0.453(1)	-0.3727(8)	2.5(5)
C(22)	0.1746(7)	0.462(1)	-0.2959(7)	2.3(5)
C(23)	0.2842(7)	0.452(2)	-0.5327(7)	2.8(6)
C(24)	-0.5640(7)	0.716(2)	-0.397(1)	5.3(7)
Cl(1)	0.4711(6)	0.776(1)	0.0870(7)	5.4(5)
Cl(2)	0.4998	0.506(1)	-0.0003	7.5(9)
Cl(3)	0.474(2)	0.888(4)	0.006(3)	9(2)
Cl(3')	0.5110(8)	0.641(3)	0.094(1)	12(1)
C(25)	0.529(2)	0.701(4)	0.026(2)	5(2)

$B_{\text{eq}} = \frac{8\pi^2}{3} \sum_{i=1}^3 \sum_{j=1}^3 U_{ij} a_i^* a_j^* \hat{a}_i \cdot \hat{a}_j$. ^be.s.d.s in the least significant figure are given in parentheses in this and succeeding Tables.

TABLE 3. Selected intramolecular distances (Å) and angles (°) for $(\text{H}_2\text{O})\text{MgT}(\text{OMe})\text{PP}\cdot\text{HCCl}_3$ from X-ray and molecular mechanics studies

	X-ray distance	MM distance
Mg-O(1)	2.078(12)	2.141
Mg-N(1)	2.084(7)	2.200
Mg-N(2)	2.088(7)	2.212
O(2)-C(14)	1.382(11)	1.367
O(2)-C(24)	1.419(16)	1.412
O(3)-C(20)	1.373(10)	1.367
O(3)-C(23)	1.431(14)	1.412
N(1)-C(1)	1.375(11)	1.380
N(1)-C(4)	1.371(11)	1.379

(continued)

TABLE 3. (continued)

	X-ray distance	MM distance
N(2)-C(6)	1.383(11)	1.386
N(2)-C(9)	1.360(11)	1.386
C(1)-C(2)	1.445(12)	1.408
C(1)-C(10)	1.402(12)	1.422
C(2)-C(3)	1.365(13)	1.394
C(3)-C(4)	1.452(12)	1.408
C(4)-C(5)	1.415(11)	1.422
C(5)-C(6)	1.388(11)	1.423
C(5)-C(17)	1.490(11)	1.432
C(6)-C(7)	1.436(12)	1.406
C(7)-C(8)	1.363(13)	1.395
C(8)-C(9)	1.426(12)	1.406
C(9)-C(10)	1.420(11)	1.423
C(10)-C(11)	1.497(12)	1.431
C(11)-C(16)	1.392(16)	1.414
C(11)-C(12)	1.387(15)	1.411
C(17)-C(18)	1.409(15)	1.414
C(17)-C(22)	1.378(15)	1.411
C(13)-C(14)	1.373(15)	1.404
C(13)-C(12)	1.403(14)	1.404
C(14)-C(15)	1.375(15)	1.405
C(15)-C(16)	1.397(14)	1.404
C(18)-C(19)	1.371(14)	1.404
C(19)-C(20)	1.388(16)	1.405
C(20)-C(21)	1.394(16)	1.404
C(21)-C(22)	1.401(14)	1.405
Average absolute difference	0.028 Å	

	X-ray angle	MM angle
O(1)-Mg-N(1)	103.0(3)	97.0
O(1)-Mg-N(2)	99.1(3)	96.2
N(1)-Mg-N(1)'	154.1(6)	167.3
N(1)-Mg-N(2)	88.1(3)	88.9
N(2)-Mg-N(2)'	161.8(6)	167.6
C(14)-O(2)-C(24)	116.2(10)	123.3
C(20)-O(3)-C(23)	116.7(10)	123.3
Mg-N(1)-C(1)	126.1(6)	121.5
Mg-N(1)-C(4)	126.6(6)	121.5
C(1)-N(1)-C(4)	106.3(7)	115.4
Mg-N(2)-C(6)	126.1(6)	122.2
Mg-N(2)-C(9)	126.6(6)	122.2
C(6)-N(2)-C(9)	107.0(7)	115.4
N(1)-C(1)-C(2)	109.3(8)	102.6
N(1)-C(1)-C(10)	126.0(8)	132.0
C(2)-C(1)-C(10)	124.7(8)	124.7
C(1)-C(2)-C(3)	108.3(8)	109.4
C(2)-C(3)-C(4)	105.0(8)	109.5
N(1)-C(4)-C(3)	111.1(8)	102.5
N(1)-C(4)-C(5)	125.4(8)	132.4
C(3)-C(4)-C(5)	123.5(8)	124.3
C(4)-C(5)-C(6)	125.6(7)	122.0
C(4)-C(5)-C(17)	117.0(7)	117.2
C(6)-C(5)-C(17)	117.3(7)	120.8
N(2)-C(6)-C(5)	125.7(8)	130.0
N(2)-C(6)-C(7)	109.5(8)	102.6

(continued)

TABLE 3. (continued)

	X-ray angle	MM angle
C(5)–C(6)–C(7)	124.7(8)	126.3
C(6)–C(7)–C(8)	106.0(8)	109.7
C(7)–C(8)–C(9)	108.1(8)	109.6
N(2)–C(9)–C(8)	109.3(8)	102.5
N(2)–C(9)–C(10)	125.3(8)	131.3
C(8)–C(9)–C(10)	125.3(8)	126.1
C(1)–C(10)–C(9)	125.2(8)	122.2
C(1)–C(10)–C(11)	117.7(8)	117.2
C(9)–C(10)–C(11)	117.2(8)	120.6
C(10)–C(11)–C(16)	121.7(11)	122.0
C(10)–C(11)–C(12)	120.9(11)	125.0
C(16)–C(11)–C(12)	117.4(8)	112.9
C(5)–C(17)–C(18)	119.9(10)	121.5
C(5)–C(17)–C(22)	121.7(10)	125.6
C(18)–C(17)–C(22)	118.5(8)	112.9
C(14)–C(13)–C(12)	116.9(10)	122.5
O(2)–C(14)–C(13)	122.7(10)	120.2
O(2)–C(14)–C(15)	115.2(11)	124.7
C(13)–C(14)–C(15)	122.0(9)	115.1
C(14)–C(15)–C(16)	119.9(10)	121.8
C(11)–C(16)–C(15)	120.5(10)	124.1
C(17)–C(18)–C(19)	119.5(10)	124.3
C(18)–C(19)–C(20)	121.8(10)	121.7
O(3)–C(20)–C(19)	115.7(11)	124.6
O(3)–C(20)–C(21)	124.5(10)	120.3
C(19)–C(20)–C(21)	119.7(9)	115.0
C(20)–C(21)–C(22)	118.0(11)	122.6
C(17)–C(22)–C(21)	122.5(11)	123.5
C(11)–C(12)–C(13)	123.3(10)	123.5
Average absolute difference	4.3°	

dimensional polymer sheet (Fig. 2). These hydrogen-bonded porphyrins are related by translational symmetry. Porphyrin macrocycles typically stack at separations of 3.4–3.6 Å in crystals, this distance being

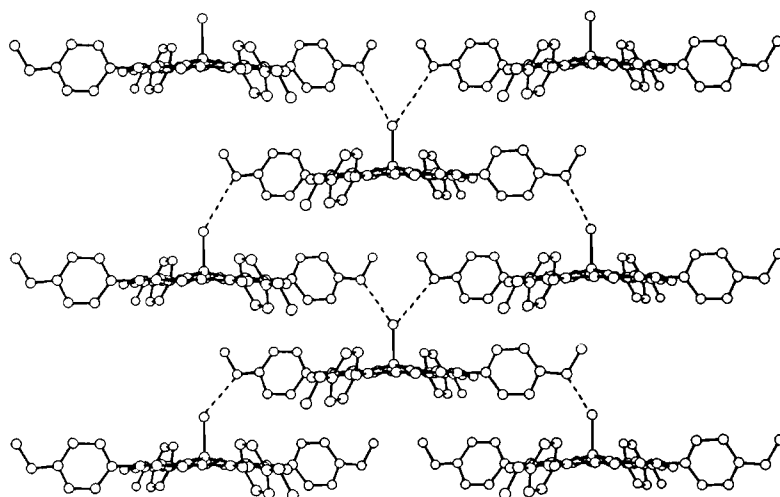


Fig. 2. Illustration of the two-dimensional polymer sheet in the structure of $(\text{H}_2\text{O})\text{MgT}(\text{OMe})\text{PP}\cdot\text{HCCl}_3$.

the optimum van der Waals contact between the π -systems of adjacent molecules. In this structure, there is no significant overlap between porphyrinato planes, although some π - π interaction may exist between the porphyrinato plane and the phenyl plane (distance ~ 3.6 Å). This hydrogen bonding aggregation system is somewhat similar to that found in the X-ray structure of ethyl chlorophyllide *a* dihydrate [1] where a one-dimensional polymer results from the formation of a hydrogen bond between the coordinated water molecule and the ketone oxygen atom of an adjacent molecule, and a two-dimensional net results from the cross-linked one-dimensional polymer caused by a hydrogen bond between the interstitial water molecule and the carbonyl oxygen atom of the ethyl ester. Fischer *et al.* [13], Strouse and co-workers [1] and recently Olson *et al.* [14] have suggested that these chlorophyll–water adducts could be used as a model for aggregation of chlorophyll *in vivo*. Katz and co-workers [15] prefer to use it as a model for a dimer in the photoreaction center. Further evidence is needed to show what is most appropriate *in vivo*. So far, crystal structures of most of the magnesium porphyrins and chlorophyll derivatives have revealed that they contain water adducts.

Molecular modeling

Modeling of an isolated $\text{H}_2\text{OMgT}(\text{OMe})\text{PP}$ via molecular mechanics gave distances and angles which were in general good agreement with those obtained from the crystal structure investigation (Table 3). The primary difference was in the orientation of the phenyl groups; in the molecular mechanics case, the dihedral angle between the phenyl rings and the porphyrin rings were found to be $\sim 35^\circ$ as opposed to the $\sim 69^\circ$ found in the crystal structure. Such a

difference is not surprising since packing effects in the crystalline state might well be expected to influence the orientation of these phenyl groups.

Molecular mechanics calculations also indicate that the hydrated form of the molecule is more stable; it is the bonding of Mg and O which plays a key role in the aggregation process.

Acknowledgments

We acknowledge our indebtedness for assistance in the synthesis of the (H₂O)MgT(OME)PP to Donald J. Czaplá. We thank Dr Mannar R. Maurya and W. S. Struve for valuable discussion. The Ames Laboratory is operated for the U.S. Department of Energy by Iowa State University under contract No. W-7405-Eng-82.

References

- 1 H.-C. Chow, R. Serlin and C. E. Strouse, *J. Am. Chem. Soc.*, **97** (1975) 7230.
- 2 M. I. Bystrova, I. N. Malgosheva and A. A. Krasnovskii, *Mol. Biol.*, **13** (1979) 582.
- 3 K. M. Smith, L. A. Kehrers and J. Fajer, *J. Am. Chem. Soc.*, **105** (1983a) 1387.
- 4 D. C. Brune, T. Nozawa and R. E. Blankenship, *Biochemistry*, **26** (1987) 8644.
- 5 A. D. Adler, F. R. Longo, F. Kampas and J. Kim, *J. Inorg. Nucl. Chem.*, **32** (1970) 2443.
- 6 *TEXSAN-TEXRAY Structure Analysis Package*, Molecular Structure Corporation, The Woodlands, TX, USA, 1985; C. J. Gilmore, *MITHRIL* an integrated direct methods computer program, *J. Appl. Crystallogr.*, **17** (1984) 42; P. T. Beurskens, *DIRDIF: Direct Methods for Difference Structure*, an automatic procedure for phase extension and refinement of difference structure factors. *Tech. Rep. 1984/1*, Crystallography Laboratory, Toernooiveld, 6525 Ed Nijmegen, Netherlands, 1984.
- 7 D. T. Cromer and J. T. Waber, *International Tables for X-ray Crystallography*, Vol. IV, Kynoch Press, Birmingham, UK, 1974, Table 2.2 A.
- 8 J. A. Ibers and W. C. Hamilton, *Acta Crystallogr.*, **17** (1964) 781.
- 9 D. T. Cromer, *International Tables for X-ray Crystallography*, Vol. IV, Kynoch Press, Birmingham, UK, 1974, Table 2.3.1.
- 10 K. E. Gilbert and J. J. Gajewski, *PCMODEL*, molecular modeling software, Version 3.0, Serenna Software, Box 3076, Bloomington, IN 47402-3076, USA.
- 11 U. Burkert and N. L. Allinger, *ACS Monograph Services*, No. 175, American Chemical Society, Washington, DC, USA, 1982.
- 12 R. Timkovich and A. Tulinsky, *J. Am. Chem. Soc.*, **91** (1969) 4430.
- 13 M. S. Fischer, D. H. Templeton, A. Zalkin and M. Calvin, *J. Am. Chem. Soc.*, **94** (1972) 3613.
- 14 J. M. Olson, G. H. Van Brakel, R. D. Gerola and J. P. Pedersen, in J. Biggens (ed.), *Progress in Photosynthesis Research*, Vol. 1, Martinus Nijhoff, Dordrecht, Netherlands, 1987.
- 15 L. L. Shipman, T. M. Cotton, J. R. Norris and J. J. Katz, *Proc. Natl. Acad. Sci.*, **73** (6) (1976) 1791-1974.